01 Jan 2023

Particulate Matter Detection In Mines Using 3D Light Detection And Ranging Technology

Zachary Osterwisch

Alexander Mauntel

Nathanael Nisbett

Dibbya Barua

et. al. For a complete list of authors, see https://scholarsmine.mst.edu/ele_comeng_facwork/4859

Recommended Citation

Z. Osterwisch et al., "Particulate Matter Detection In Mines Using 3D Light Detection And Ranging Technology," *IEEE Wireless Communications and Networking Conference, WCNC*, Institute of Electrical and Electronics Engineers, Jan 2023.
The definitive version is available at https://doi.org/10.1109/WCNC55385.2023.10118999

Particulate Matter Detection in Mines Using 3D Light Detection and Ranging Technology

Zachary Osterwisch[1], Alexander Mauntel[1], Nathanael Nisbett[1], Dibbya Barua[1], Ahmad Alsharoa[1]
[1]Missouri University of Science and Technology, Rolla, MO, USA

2023 IEEE Wireless Communications and Networking Conference (WCNC) | 978-1-6654-9122-8/23/$31.00 ©2023 IEEE | DOI: 10.1109/WCNC55385.2023.10118999

***Abstract*—This paper proposes a novel portable prototype and self-contained Air Quality (AQ) monitoring device that utilizes Light Detection and Ranging (LiDAR) technology to take its measurements. The novel device aims to improve mining safety by collecting and analyzing the AQ inside mines and displaying the real-time conditions to personnel. The intent is to create a 3D map of the environment and display potentially hazardous Atmospheric Particulate Matter (APM). To achieve this goal, we prototype a portable, compact, and easy-to-operate system that utilizes LiDAR to detect APM. Then, we propose how the collected data can be used to calculate real-time AQ conditions. Finally, we illustrate selected results to show the importance and feasibility of our novel prototype.**

***Index Terms*—Light Detection and Ranging (LiDAR), Atmospheric Particulate Matter (APM), Real-time 3D Map.**

I. Introduction

Air quality (AQ) monitoring is a crucial aspect of the mining industry and defines the amount of pollutants in the air. AQ is typically measured in units of mass of the pollutant per volume of air [1]. Dust is typically released into the air of a mine during the extraction, transportation, and processing of minerals. This dust, or Atmospheric Particulate Matter (APM), can be classified into two categories of concern based on size: float dust with diameter sizes $\leq 70\mu$m, and respirable dust with diameter sizes $< 10\mu$m [2], [3].

Float dust is a concern because it poses an explosion threat in underground mines, while respirable dust is a direct danger to the miners' health because it can lead to diseases [2]. Inhaling float coal dust can lead to Coal workers' Pneumoconiosis (CWP), commonly known as black lung disease [3]. CWP is a disabling and potentially fatal lung disease, and it has a tremendous human and financial toll on the US coal mining industry. Float silica is another potential danger that can lead to silicosis, also a disabling lung disease. The most severe form of these diseases, Progressive Massive Fibrosis (PMF), is also fatal [4]. Data from The National Institute for Occupational Safety and Health suggests that both the prevalence of CWP and PMF have increased since 2000 [4].

One of the best ways to reduce APM exposure is to better monitor the AQ inside mines. Light Detection and Ranging (LiDAR) technology has the potential to help monitor AQ. This technology operates by utilizing laser technology to cast multiple laser beams across a Field-of-View (FoV) area, measuring the time it takes for the return signal, and then calculating the distance between the sensor aperture and the object the laser beams hit [5]. This data can be used to generate precise and real-time 3D maps that can be used for several applications such as surveying, wildfire detection, autonomous vehicles, human detection, etc [5], [6]. Although cameras can take high-resolution pictures, they are not able to provide accurate spatial information unlike LiDAR sensors, which can measure object dimensions and distances between objects. Furthermore, LiDAR can work under different lighting situations while cameras do not perform well in low-light situations, such as those in mines [7].

An important part of AQ monitoring in mines is to measure how APM moves through the air and spatially locate the APM inside the mines. This area of concern has resulted in numerous solutions to assist with the problem, but each of them has its own set of disadvantages. The biggest downfall for AQ solutions in the industry is that they are single-point sensors [8]. These sensors only provide the AQ at the location of the sensor and cannot visualize the spatial movement of APM. Further, some AQ monitoring technology is designed to measure only one APM size, such as PM2.5 or PM10 (PM10 = APM diameter 10μm) [12]. Lastly, a lot of these sensors are not portable, and therefore, a large number of sensors are required inside the mine to track and monitor APM.

Real-time monitoring is an important aspect of AQ monitoring because the APM is harmful and potentially lethal for mine workers. To mitigate risk and protect workers, the on-site personnel should be alerted in real-time if APM levels were too high. However, some traditional compliance monitoring in the mining industry can be slow. The process involves sampling, collection, and then sending the collected sample off for analysis [9]. This process can take hours, days, or sometimes weeks to get results back. Although devices like Aeroqual Dust Sentry [10] do not require their samples to be sent off, the given results are a 24-hour average. These sensors also require added maintenance, and thus added cost, because their filters need to be changed daily or weekly.

There have been few works in literature about LiDAR-based detection methods for APM in the mining industry. The work in [13], proposed to use stationary micro-pulse LiDAR at above-ground mines to track large plumes of dust for up to 6 kilometers. However, this would only be applicable for above-ground mines and for large plumes of APM which is not of concern in this paper. The contract in [14] discusses the goal of dust detection in mines using LiDAR technology, and it lists the potential benefits that LiDAR could provide, but it is only a proposal for the idea. Both these sources propose the idea and potential benefits LiDAR could provide for dust detection, but they both did not define a method for detection or design a prototype to test the technology. The work in [15] utilizes LiDAR's mapping ability to track and estimate mining subsidence, not AQ monitoring.

To the best of our knowledge, current LiDAR solutions

Current Solutions	Functionality	Drawbacks
Aerodynamic Particle Sizer (ex. TSI 3321) [8]	High-resolution real-time aerodynamic measurements of particles from 0.5μm to 20μm	- Very Large - Needs flowing air - Provides data only from a single collection point
High Volume Air Sampler (ex.Partisol 2000i-D) [9]	Measures the AQ of a large area, typically >1500 m^3 of air over a period of 24 hours. Dust filter must be changed daily and sent to the lab to be analyzed	- Does not indicate time of contamination - Laboratory analysis required - Analysis could take weeks
Real-Time Dust Monitoring (Ex. Dust Sentry PM2.5 Monitor) [9] [10]	Monitors dust in the air minute by minute and can send updates to the selected people that alert them when dust levels go beyond a certain level	- Typically large and not easily movable - Very expensive (∼$10,000) - Only measures AQ at a single point
Hand-Held Particle Monitoring Devices (Ex. Fluke 985 Particle Counter) [11]	Monitors dust particles in the air from a single point. Extremely portable and accurate measurements of particle concentrations	- Expensive (∼$5000) - Only measures AQ at a single point

TABLE I: Current AQ solutions and advantages of LiDAR technology.

inside mines are not used for AQ monitoring. In this paper, we propose for the first time a portable, self-contained AQ monitoring device that utilizes LiDAR technology and will focus on prototype development to demonstrate proof of concept. In Table 1, we compare the discussed current solutions with our proposed solution.

II. System Model

This section outlines the general hardware required for our proposed portable AQ monitoring device and then explicitly states the hardware used in our prototype.

A. Hardware and Operation

The operation of this device relies on two main components: a LiDAR sensor and a mini-computer. LiDAR is used to scan the environment and collect data, and the computer is responsible for data processing, storage, and running the AQ algorithms. Other important components of this design include peripherals to interact with the computer, such as a monitor and keyboard, and a power supply large enough to power the unit for several hours. Lastly, all these components will need to be mounted on a portable object that can be moved with ease. This paper focuses on the physical prototype and the intended future operation procedure.

The portable AQ LiDAR device will be moved to an area of interest during normal atmospheric conditions, that is to say, without an abundance of APM. The calibration process involves the LiDAR scanning the environment to establish a baseline and the operator choosing the APM they would expect the LiDAR to measure. Choosing the APM is an important step because AQ requires the mass of the pollutant, and different pollutants have different masses associated with them. Once the device is properly calibrated, it will continuously monitor the AQ in real-time. The monitor will show the 3D point cloud of the environment and will box any APM. The box colors will be green, yellow, and red depending on the concentration of APM. Safe levels of APM are boxed in green, warning levels are boxed in yellow, and unsafe levels are boxed in red.

B. Prototype

Fig. 1 shows the designed prototype with labeled components. At the top is a Livox LiDAR sensor which sits in a 3D-printed mount. Two LiDAR sensors were used in testing, Livox Mid-40 and Livox Tele-15, and both sensors utilize a wavelength of 0.905μm [16]. This wavelength should

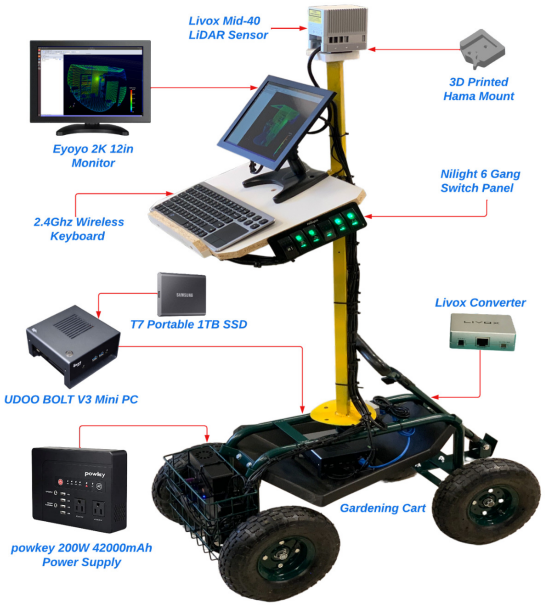

Fig. 1: Prototype of portable AQ LiDAR device.

theoretically allow the sensor to confidently detect APM which is of concern in the mining industry. Fig. 2 shows the type of scattering based on the size parameter x, which is a ratio based on the size of the measured particle and the wavelength. The two LiDARs use a wavelength that should produce Mie Scattering when interacting with APM diameter size $< 10\mu$m. This type of scattering is the same type produced by current AQ sensors during the calculation of their single-point AQ measurements [8], [10].

The use of different LiDAR sensors will be discussed in Section III. Under the LiDAR is the user station which includes the 2k 12" monitor, a wireless keyboard and touchpad, and a 6-gang switch panel. The monitor and keyboard are used for operator interaction with the mini-PC and LiDAR. The switch panel is wired so that the LiDAR, mini-PC, and monitor are on isolated circuits and can be controlled separately. Sitting on the bottom of the cart is a UDOO Bolt V3 mini-PC and an external Samsung 1TB SSD as its storage unit. The choice of UDOO is due to its Linux operating system, CPU architecture, dedicated Radeon GPU, and DDR4 RAM. These components would allow the PC to quickly calculate the AQ algorithms. An ethernet cable from the mini-PC and a power cable plugs into the Livox Converter. The Converter combines these signals and feeds them to the LiDAR sensor. A 42,000 mAh portable

power supply is responsible for powering all the devices for approximately 6-8 hours before needing a recharge. Lastly, all the components are mounted on a portable gardening cart that was retrofitted for these specific parts. The prototype, including both LiDAR sensors, costs approximately $2,600.

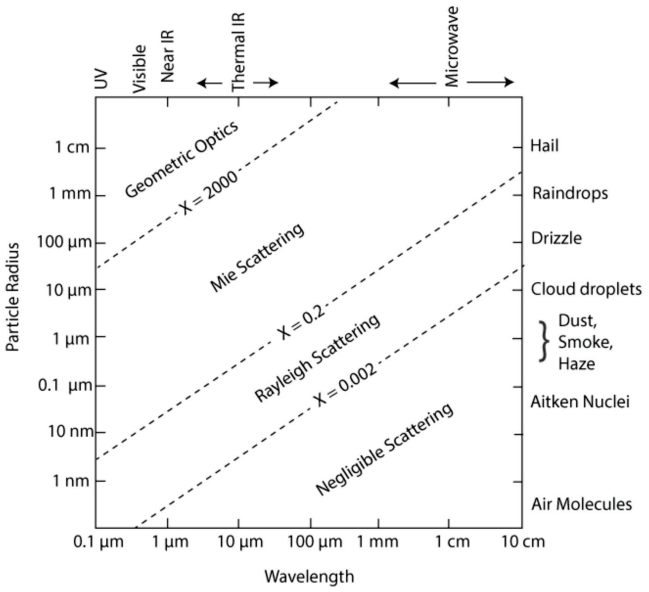

Fig. 2: Scattering regimes depending on wavelength, $x \equiv \frac{2\pi r}{\lambda}$ [17].

III. Experimentation

In this section, we describe three major experiments our prototype underwent, explain the purpose of each test, and discuss the test results. The visual representation of LiDAR data is called a point cloud. Every data points represent a physical location in 3D space, and a collection of points can be used to identify objects. All LiDAR data also has a reflectivity value associated with its spatial attribute. The reflectance value represents how much power from the initial laser pulse was received by the LiDAR upon its return, and this value is typically represented within a range of colors. A low reflectance means a laser pulse returned to the sensor with much less power than it started with. For this paper, Fig. 3 shows how LiDAR point cloud data will be displayed, and the reflectivity gauge is the same color scale that will be used for all LiDAR data. Data points in a point cloud that have colors closer to red are more reflective, while colors closer to blue are less reflective. The Reflectivity gauge numbers 0 to 150 correspond to the reflectivity within the range of 0 to 100% in the Lambertian reflectance model. Values of 151 to 250 correspond to objects with retroflection properties [16].

A. Whiteboard Reflectivity Experiment - Proof of Concept

1) Description: The first test performed was a reflectivity experiment using a whiteboard. This test aimed to discover if APM was detectable by a LiDAR sensor. We had three theories about how the APM would appear in LiDAR's point cloud data. Theory one: the APM is large enough to reflect all of the light from a single laser pulse. Theory two: the APM is small enough to reflect part of a laser pulse while the rest would continue to a surface beyond the APM before reflecting back to the sensor. Theory three: the APM is too small for the LiDAR's laser beam to interact with. Theories one and two would produce reflectivity values drastically lower than the reflectivity values of the whiteboard and prove that APM was detectable by LiDAR. Theory three would mean the test was unsuccessful and LiDAR could not be used to detect APM.

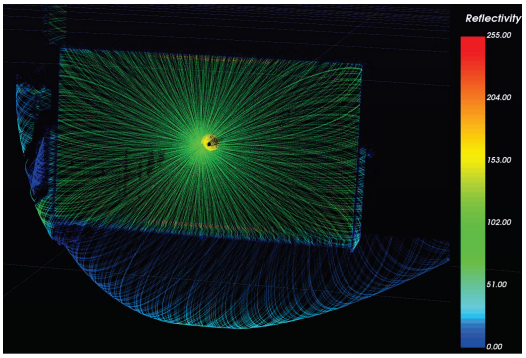

Fig. 3: Whiteboard Reflectivity baseline point cloud data.

The APM chosen for this initial test was talcum powder, and it had a median diameter of 26.57 μm [18]. Based on Fig. 2, theory one or two are the expected results. The sensor used for this test was a Livox Mid-40 LiDAR sensor and has the specifications of 100,000 points per second with a circular FoV of 38.4°. The test was conducted by first aiming the LiDAR sensor at a blank whiteboard and recording data without any APM. After baseline data was collected, talcum powder was introduced into the environment. Three separate deposits of talcum powder were added to the environment throughout the test.

2) Results: Fig. 3 shows the baseline point cloud data of the whiteboard without APM in the environment. The reflectivity values of whiteboard data points were in the range of 80 and above and appeared greener. Talcum powder was then introduced into the environment in three separate deposits. The reflectivity values were charted from the start of the experiment until after the last talcum deposit. Reflectivity values were averaged in intervals of 25ms. While the whiteboard had a lot of green data points in the baseline and represents values above 80, the average reflectance was calculated using the entire FoV.

The average reflectivity values of the LiDAR data decreased from the baseline after the talcum powder was deposited, and each of the three deposits caused the average reflectance to decrease further. These results are plotted in the graph in Fig. 4. As mentioned, because all the data points were averaged at intervals of 25ms, the baseline average at the beginning of the test was around 60. The three talcum deposits are distinctly identifiable on the figure at the 5, 20, and 40-second marks. The average reflectance values dramatically decreased at each deposit, and then the values slowly increased as the powder dispersed until the next deposit occurred. The point cloud data of the environment after the three deposits are shown in Fig. 5.

This test was successful at proving a LiDAR sensor could detect small APM, such as talcum powder. However, the data was inconclusive in determining if the APM reflected all of the light from a single pulse, or if the APM reflected only part of the light. Also, even though the test was successful, talcum powder has a diameter larger than respirable dust APM, which

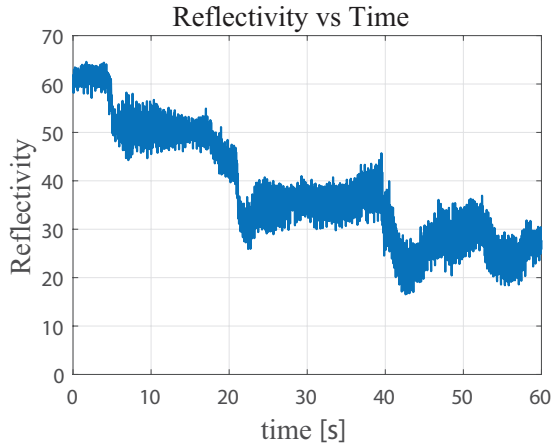

Fig. 4: Average reflectance during Whiteboard Reflectivity Experiment.

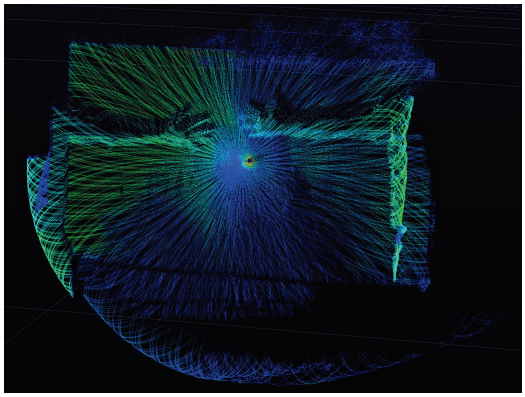

Fig. 5: Whiteboard Reflectivity point cloud data with talcum powder.

is of concern in mines. Further experimentation is required to determine if LiDAR can spatially detect a cloud of APM and if LiDAR can detect APM as small as those found in mines.

B. Wind Tunnel Experiment - Verify APM Size

1) Description: The next major experiment was conducted at the Missouri S&T Experimental Mine Wind Tunnel in the Mining Department. The intent of this experiment was to discover the limits of the Mid-40 LiDAR's capabilities in detecting small APM. The Whiteboard Reflectivity Experiment, described in Section III-A, discovered LiDAR could detect APM with a diameter of approximately 26.57 μm. However, in the mining industry, respirable dust APM, with diameter < 10 μm, are the main hazardous concern for workers [19]. The wind tunnel provided the ability to control the size of the APM.

The experiment used respirable coal dust APM, which has an average diameter size of < 10 μm. An overhead view of the setup is shown in Fig. 6. The coal dust entered one end of the wind tunnel and was blown through the tunnel toward the LiDAR sensor. The large distance between the input point and the sensor gave the coal dust ample opportunity to diffuse through the air in the tunnel. The test began with no APM in the environment before introducing the coal dust. Coal dust was introduced into the wind tunnel in two deposits. The first deposit had the coal dust enter the wind tunnel with the fans

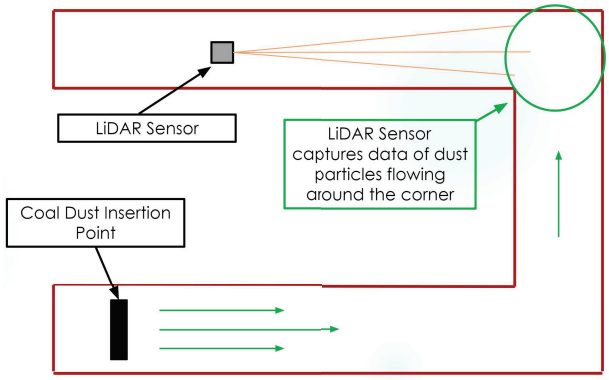

Fig. 6: Wind Tunnel Experiment setup.

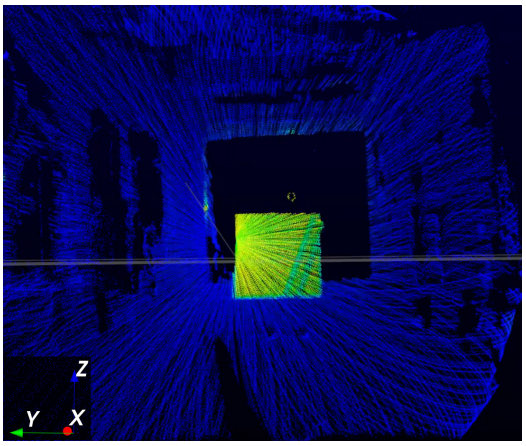

Fig. 7: Wind Tunnel baseline point cloud test data.

on high, and the second deposit of coal entered the tunnel, and then the fan was turned off.

2) Results: The baseline point cloud data of the environment before the coal dust was introduced can be seen in Fig. 7. The higher reflectivity object in the center, the yellow-green square, was a cardboard box placed in the tunnel. The walls of the tunnel were clear plexiglass, and the transparent material caused the LiDAR laser beams to pass directly through the back of the tunnel. The cardboard box provided a nontransparent and reflective surface for the LiDAR to reflect off. The lower reflectivity data, the dark blue data points, are the walls of the plexiglass tunnel. These data points were not used in the analysis. Only the data points that fell within the y and z coordinates of the cardboard box were used for calculations.

Fig. 8 plots the reflectivity versus time for this experiment. Similar to the Whiteboard Reflectivity Experiment, the reflectivity was reduced as a result of the LiDAR's light reflecting off the APM. The first deposit of coal dust when the fans were on high saw a sharp decrease in the reflectivity values before returning to a higher value. This bounce in values happened because the fan in the tunnel quickly blew the coal dust out the other end. After the second deposit of coal dust, the fan was turned off. Turning off the fan allowed the LiDAR to capture data as the APM was suspended in the tunnel. Fig 9 is the point cloud data when reflectivity was at its minimum. The LiDAR detected the fine APM as it floated in the tunnel, and it took more than two minutes for the reflectivity values to return to $\sim$70% of their original value. The team hypothesized

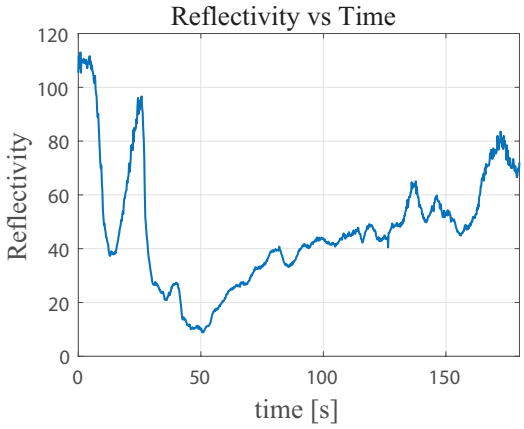

Fig. 8: Wind Tunnel reflectivity vs time with coal dust.

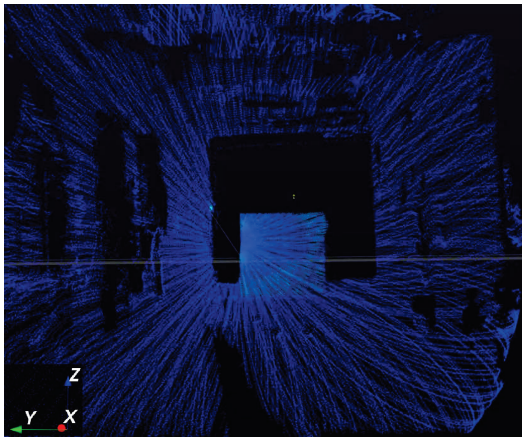

Fig. 9: Wind Tunnel point cloud test data with coal dust.

that the reflectivity values slowly increased because some coal dust settled on the bottom of the wind tunnel while some coal dust became homogeneously mixed in the tunnel and thus decreased concentration in front of the cardboard.

Another question of concern was, could the LiDAR spatially detect the APM? If reflectivity values decreased, but the data points still lay directly on the surface of the cardboard, that would mean the APM was only reflecting some of the LiDAR light and the surface behind the APM was reflecting the rest. If the reflectivity dropped but the data points were in front of the cardboard, that would mean light was reflecting off of the APM. Fig. 10 is a graph of the x distance standard deviation versus time. The decrease in distance deviation values with respect to the x direction correlates to reflectivity decreases in Fig. 8. This correlation between Fig. 8 and 10 would indicate that LiDAR detected a small spatial change in the data as reflectivity values decreased due to the APM. The results of this experiment proved that LiDAR can detect APM with diameter sizes of < 10 μm and can spatially identify the APM.

C. Outside Wall Experiment - Spatially Detect APM

1) Description: This third and last experiment was needed because of uncertainty in the previous experiment. Although LiDAR could return spatial data of the APM, there was a chance that the light beams were partially reflecting off the APM, and the rest of the light was reflecting off a surface beyond the APM. A LiDAR sensor with a double-return feature could potentially capture this data. A double-return

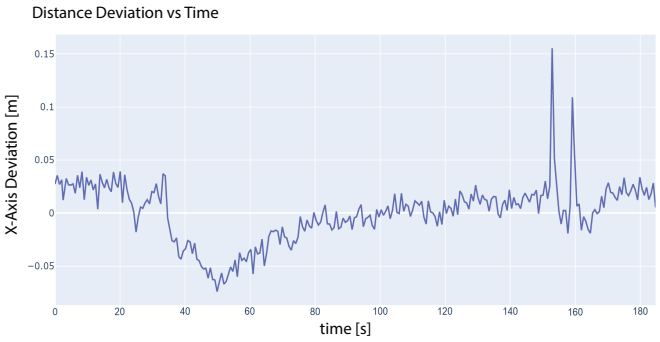

Fig. 10: Wind Tunnel distance deviation vs time with coal dust.

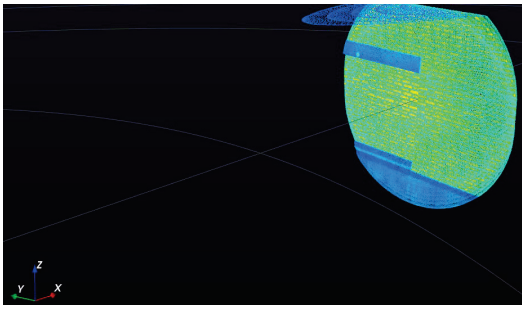

Fig. 11: Tele-15 Outside Wall baseline point cloud data.

data point is when a LiDAR can record two separate returns from a single light beam. The Livox Mid-40 sensor, used in previous experiments, did not have the double-return capabilities. Therefore, a more sophisticated sensor was required for this test. The Livox Tele-15 had the double-return feature required, and it had the added benefit of providing four times the amount of data points per second than the Mid-40. The only drawback was that the Tele-15 had a much smaller FoV. The smaller FoV required consideration while setting up the experiment but it did not negatively impact the results.

The test was set up by aiming the Tele-15 LiDAR sensor at a brick wall outside, and it was set up several meters away due to the smaller FoV. Since there was wind outside to account for, the APM was deposited only once and outside the sensor's FoV on one side. The wind then carried and dispersed the APM across the LiDAR's FoV. Talcum powder was used as the APM due to its easier access, simpler clean-up, and safer to use.

2) Results: The baseline for this experiment is shown in Fig. 11. The brick wall is the lighter reflectivity data on the right side, and the extra points per second from the Tele-15 provided a higher resolution point cloud. The talcum powder was deposited after the baseline data was collected.

Fig. 12 shows the point cloud data of the wall with the APM suspended in front of it. The LiDAR sensor was able to capture data points of the APM and also data points of the wall behind the APM. As the talcum powder passed in front of the wall, the reflectivity values dropped. From these results, we concluded the LiDAR was receiving double-return data points. The sensor's pulses of light partially reflected off the APM, while the rest of the light continued toward the wall. The remaining light then reflected off of the wall and returned to the sensor. However, since the light lost some power when

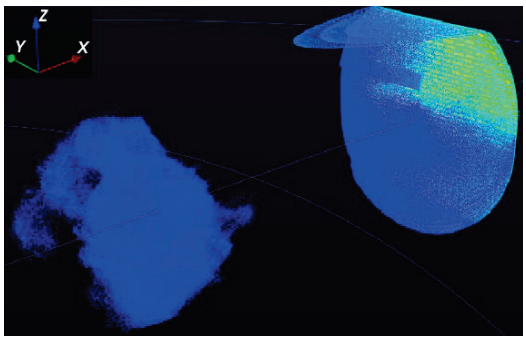

Fig. 12: Tele-15 Outside Wall point cloud data with APM.

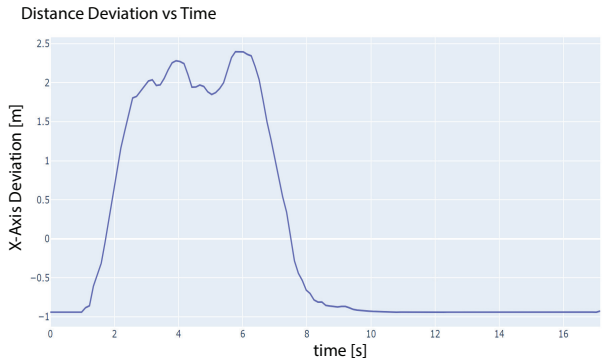

Fig. 13: Outside Wall distance deviation vs time with APM.

it first reflected off the APM, the reflected light from the wall had much less power than it started with. This lesser power is why the data points on the wall also had low reflectivity while the APM was in front. Higher reflectivity data points can be seen in Fig. 12 on the top right section of the wall. These points had a higher reflectivity because the sensor's light did not pass through any APM.

An important figure that was generated from the outside wall point cloud data can be seen in Fig. 13. Similar to Fig. 10 from Section III-B, this is a graph of the x distance standard deviation versus time. As APM moved across the FoV of the sensor, and data points were recorded both at the APM location and the wall that lay beyond, the standard deviation increased. As the wind blew the APM out of the FoV, the distance deviation in the data points decreased and returned to normal. The importance of this factor will be discussed further in Section IV. In conclusion of this section, the experiment was successful with respect to LiDAR being able to detect APM spatially.

IV. Conclusion

This paper designed a portable and self-contained AQ monitoring prototype that utilizes LiDAR technology to detect APM. The prototype underwent multiple experiments with different LiDAR sensors to verify its potential to detect APM. The Mid-40 LiDAR successfully detected both large and small APM, and the more powerful Tele-15 LiDAR spatially detected APM without losing the environment data beyond the APM. This enhances mining safety by displaying and analyzing APM in a real-time 3D map. Future extensions to this work can focus on proposing adequate artificial intelligence AQ algorithms taking into consideration the reflectivity, distance deviation, and the number of reflected data points.

V. Acknowledgements

We would acknowledge Dr. Guang Xu, an Associate Professor in the Mining Engineering Department at the Missouri S&T. He provided insights into mining ventilation and allowed us to perform experiments at the Experimental Mine Wind Tunnel.

References

[1] S. K. Malyan, O. Kumar, R. Ranjan, and J. Kumar, "Understanding units of measurement in agricultural and environmental science," *International Journal for Environmental Rehabilitation and Conservation*, vol. 9, no. 2, p. 45–51, Dec. 2018.

[2] C. E. Seaman, M. R. Shahan, T. W. Beck, and S. E. Mischler, "Design of a water curtain to reduce accumulations of float coal dust in longwall returns," *International Journal of Mining Science and Technology*, vol. 30, p. 443–447, Sep. 2020.

[3] J. F. Colinet, "The impact of black lung and a methodology for controlling respirable dust," *Mining, Metallurgy, & Exploration*, vol. 37, no. 6, p. 1847–1856, Feb. 2020.

[4] The National Institute for Occupational Safety and Health and Centers for Disease Control and Prevention, "Mining topic: Respirable dust," Oct. 2020.

[5] M. C. Lucic, H. Ghazzai, A. Alsharoa, and Y. Massoud, "A latency-aware task offloading in mobile edge computing network for distributed elevated LiDAR," in *Proc. of the IEEE International Symposium on Circuits and Systems (ISCAS), Seville, Spain*, pp. 1–5, Oct. 2020.

[6] D. Rjoub, A. Alsharoa, and A. Masadeh, "Early wildfire detection using UAVs integrated with air quality and LiDAR sensors," in *Proc. of the IEEE Vehicular Technology Conference Workshops (VTC-Fall), London, UK*, pp. 1–5, Sept. 2022.

[7] P. Wang, "Research on comparison of LiDAR and camera in autonomous driving," *Journal of Physics: Conference Series*, vol. 2093, pp. 12–32, Nov. 2021.

[8] TSI, "Aerodynamic particle sizer (APS) 3321." Accessed: Sept. 2022.

[9] Aeroqual, "Why monitor mine, construction and quarry dust in real-time?," Dec. 2021.

[10] Aeroqual, "Aeroqual dust sentry PM2.5." Accessed: Sept. 2022.

[11] Fluke, "Fluke 985 particle counter." Accessed: Sept. 2022.

[12] Gas Sensing, "Aeroqual dust sentry dust monitor." Accessed: Sept. 2022.

[13] Droplet Measurement Technologies, "Mining emissions effectively monitored with micro pulse LiDAR technology," Jun. 2020. Accessed: Sept. 2022.

[14] Center for Disease Control and Prevention, "Mining contract: LiDAR technology adaptation to underground coal mines for float coal dust and rock dust mapping applications," Aug. 2016.

[15] H. Yu, X. Lu, G. Cheng, and X. Ge, "Detection and volume estimation of mining subsidence based on multi-temporal lidar data," in *proc. of the 19th International Conference on Geoinformatics, Shanghai, China*, pp. 1–6, June 2011.

[16] Livox Technology Company Limited, *Livox Mid Series User Manual*, Aug. 2019.

[17] S. Stuke, *Characterizing thin clouds using aerosol optical depth information*. PhD thesis, Nov. 2016.

[18] C. R. Gilbert, B. R. Furman, D. J. Feller-Kopman, and P. Haouzi, "Description of particle size, distribution, and behavior of talc preparations commercially available within the United States," *Journal of Bronchology and Interventional Pulmonology*, vol. 25, no. 1, p. 25–30, Jan. 2018.

[19] L. Pan, S. Golden, S. Assemi, M. F. Sime, X. Wang, Y. Gao, and J. Miller, "Characterization of particle size and composition of respirable coal mine dust," *Minerals*, vol. 11, no. 3, Mar. 2021.